



Results of the 10th year PCCV ISI at Tsuruga Unit No.2

Yukio Watanabe¹⁾, Asao Kato¹⁾, Ikuro Kawai¹⁾, Tsuneo Yamaguchi²⁾ and Mikio Yamamoto³⁾

1) *The Japan Atomic Power Company, Japan*

2) *Obayashi Corporation, Japan*

ABSTRACT: The 10th year ISI to confirm the tendon tensile force was enforced last year on the Tsuruga Unit No.2 which has the longest running experience in Japan adopting the PCCV. This paper reports the test and the evaluation results obtained from the 10th year ISI.

From the 10th year ISI results compared with the 5th year ISI results, enlargement of concrete cracks were not found and grease leaks did not occur. Also, the declining ratio of tendon tensile force with time at both the dome portion and the cylinder portion dwindle.

The evaluation on the declining amount of tendon stress reduced was made based on the equation on creep, drying shrinkage of concrete in the standard¹⁾ by Japan Society of Civil Engineering revised. Measurements of both concrete strain and residual tensile force of tendon corresponds well with the calculations. From these results the structural integrity of the PCCV at Tsuruga Unit No.2 was confirmed to be secure.

1. INTRODUCTION

Tsuruga Unit No.2 is in its 12th year of operation this year, which has the longest operating experience in Japan adopting the PCCV method. Since the start of construction in April 1982, the SIT has been enforced in February 1986, C/O in February 1987, the first year ISI in January 1988, the 3rd year ISI in August 1990, the 5th year ISI in May 1993 and the 10th year ISI September 1998. After the SIT periodical inspection, concrete strain and the temperature of the PCCV have been measured 2 times a year and also lift-off tests at ISI are performed to obtain the residual tensile forces at the tendon ends.

2. OBJECTIVE

The objective of this paper is to discuss the adequacy of the evaluation methods used on PCCV in Japan and the maintenance of PCCV's structural integrity from the measurement and evaluation results indicated by all kinds of measurements and evaluations made on the PCCV in the past 12 years.

3. DIMENSIONS OF THE PCCV

The dimensions of the Tsuruga Unit No.2 is shown in Fig. 1. The upper structure of the PCCV is formed by a 1.3m thick cylindrical wall with height and inner diameter of 43.0m and over it a 1.1m thick hemispherical dome of 21.5m inner radius. At the bottom portion is a 8.0m thick

foundation mat and a 6.4mm steel liner covering the inner surface of the upper structure and the bottom to ensure leak prevention functions.

The 1,000ton class BBRV (un-bonded) is adopted as the prestressing system where the hoop tendon is anchored to the 3 buttresses located in the circumferential direction and the vertical inverted U tendon to the tendon gallery within the foundation mat.

4. OUTLINE OF ISI PRACTICE

Inspection and test items listed hereunder for the ISI are enforced in conformity with the US 10CFR50.

- Visual inspection of exposed concrete, anchoring portion of tendon and its surrounding concrete
- Inspection and chemical testing on extracted grease and newly injected grease
- Measuring of tendon lift-off force

The time of enforcement is 1, 3, 5, and 10 years after commercial operation. The tendons inspected are divided into two groups, inverted U tendons and hoop tendons from which 4% and 4 at minimum are randomly chosen for testing. And of them 1 from each group shall be tested from the first ISI throughout the plant life to clarify its history and compare with its past observed data. Moreover if there has not been any abnormality in the past three tests, the number of specimen from the fifth year is reduced to 2% and 3 at minimum of the entire number from each groups.

Abnormality has not been found in the 10th year ISI results which is the same as previously performed tests.

5. CONCERNS WITH CONCRETE STRAIN

1) Concrete Strain Measurement Methods

Concrete strain and temperature has been measured periodically 2 times a year, in the summer and winter after the SIT. The locations of strain measurement are shown in Fig.1.

Strain was measured by a total of four strain gauges embedded in both inside and outside the concrete wall for longitudinal or circumferential direction per one measurement section. Each strain measurements include thermal strain which is accompanied by the temperature changes within the section. Therefore, temperature at 3 to 5 points for each measurement section were used to estimate the approximate thermal strain which were eliminated from the measured strain. The strain measurement after the elimination of thermal strain was used as strain measurements and are indicated after converting them into membrane strain of each section in the longitudinal and circumferential directions.

2) Measurement Results and Evaluation of Concrete Strain

When designing the PCCV structure, creep and drying shrinkage strain are calculated based on the standard¹⁾ by Japan Society of Civil Engineering which conforms to the CEB-FIP CODE 1978. The author uses the creep and drying shrinkage equations revised as below for evaluation²⁾.

① Consideration of humidity fluctuation due seasonal changes

The design creep factor and drying shrinkage strain for structural design is described as Eq.(1) and (2) respectively. The periodical fluctuation of strain at the PCCV concrete structure is understood to be due to seasonal changes in humidity and its characteristics can be expressed with the use of the sine function. Within this, the basic creep factor(ϵ_{cs}) and basic shrinkage

strain (ϵ_{s0}) is assumed to amplify as the sine function with a width of $\pm 10\%$ based from the value (A, B) of the standard ²⁾ indicated above and are described as Eq.(3) and (4) .

$$\phi(t, t_0) = \phi_{d0} \cdot \beta_d(t - t_0) + \phi_{f0} [\beta_f(t) - \beta_f(t_0)] \quad \dots (1)$$

$$\epsilon_{cs}(t, t_0) = \epsilon_{s0} [\beta_s(t) - \beta_s(t_0)] \quad \dots (2)$$

$$\phi_{f0} = A + A/10 \times \text{Sin} \left[2\pi(t - t_0 + \Delta t') / 365 \cdot C \right] \quad \dots (3)$$

$$\epsilon_{s0} = B + B/10 \times \text{Sin} \left[2\pi(t - t_0 + \Delta t') / 365 \cdot C \right] \quad \dots (4)$$

Here, t_0, t : is the effective age (days) of the concrete at time of loading and at the time of evaluation respectively which is calculated from $\Sigma(T+10) \cdot \Delta t' / 30$. T : temperature($^{\circ}\text{C}$), $\Delta t'$: number of days when the temperature is $T^{\circ}\text{C}$, $\Delta t'$: multiplication of coefficient C of effective material age and the number of days between the standard day (Oct. 1) and the day of loading, C : coefficient of effective material age $(T+10)/30$, A : coefficient decided from relative humidity conditions (when humidity is 70% the factor is 1.80 and at 80% is 1.50 with adjustment), B : coefficient decided from relative humidity conditions (when humidity is 70% the factor is 227 and at 80% is 164 with adjustment).

② Biaxial stress effects are considered together with effects due to section loss by tendon, reinforcement, steel liner and tendon ducts, and are reflected to the concrete elastic modulus.

Evaluation formulas of creep strain and drying shrinkage strain are as follows.

$$\epsilon_{creep}(\theta) = \phi(t, t_0) \cdot \epsilon_{\theta} \quad ; \epsilon_{\theta} = (\sigma_{\theta} - \nu_c \cdot \sigma_{\phi}) / E_c \quad \dots (5)$$

$$\epsilon_{creep}(\phi) = \phi(t, t_0) \cdot \epsilon_{\phi} \quad ; \epsilon_{\phi} = (\sigma_{\phi} - \nu_c \cdot \sigma_{\theta}) / E_c \quad \dots (6)$$

$$\epsilon_s = \epsilon_{cs}(t, t_0) \quad \dots (7)$$

Here, $\phi(t, t_0)$: creep coefficient considering the seasonal fluctuations of humidity, ν_c, E_c : equivalent Poisson's ratio and equivalent elastic modulus of concrete, $\epsilon_{cs}(t, t_0)$: drying shrinkage strain considering the seasonal fluctuations of humidity.

Representative examples of concrete strain measurement results and evaluation results of the total strain of creep and drying shrinkage are shown in Fig. 2 to 4. Here the horizontal axis is the effective age t since concrete placement and the vertical axis is the amount of changes in strain ϵ since the start of SIT. As can be seen from the figures, the measured strain correspond well with the amended equation.

6. THE RESIDUAL TENDON FORCES

The layout of tendons within the PCCV is shown in Fig.5. The measurement of tensile force at tendon ends were performed with the use of filler gauges and the average of the 3 measurements is set as the lift-off force at tendon ends. Equations in the standard¹⁾ by the Japan Society of Civil Engineering in Table 1 are used for calculating design tensile force, where elastic loss of concrete (ΔF_e) is calculated by FEM method and creep loss (ΔF_c) and drying shrinkage loss (ΔF_s) of concrete uses Eq. (5) to (7) indicated in the previous paragraph on evaluation method of strain for the evaluation of tensile force at tendon ends. Furthermore,

relaxation loss (ΔF_2) is calculated with the same equation as for design.
 The evaluation equations (details are in reference 2)) of tendon tensile force are indicated in Table I.

Table 1 Design Equations and Evaluation Equations for Tendon Tensile Force

Design Equation	elastic deformation loss (tf)	$\Delta F_1 = A_p \cdot \frac{1}{2} \cdot n \cdot \sigma_c$
	relaxation loss (tf)	$\Delta F_2 = A_p \cdot \Gamma(t) \cdot f_i \left(1 - 2 \times \frac{\Delta F_3 + \Delta F_4}{f_i} \right)$
	creep loss (tf)	$\Delta F_3 = A_p \times \frac{n \times \phi(t, t_0) \times \sigma_c}{1 + n \times \frac{\sigma_c}{f_i} \left[1 + \frac{1}{2} \phi(t, t_0) \right]}$
	drying shrinkage loss (tf)	$\Delta F_4 = A_p \times \frac{E_p \times \epsilon_s(t, t_0)}{1 + n \times \frac{\sigma_c}{f_i} \left[1 + \frac{1}{2} \phi(t, t_0) \right]}$
Proposed Evaluation Equation	elastic deformation loss (tf)	$\Delta F_1 = E_p \cdot A_p \cdot \Delta \epsilon$
	relaxation loss (tf)	$\Delta F_2 = \Gamma(t) \cdot F_0 \cdot \left\{ 1 - 2 \times (\Delta F_3 + \Delta F_4) / F_0 \right\}$
	creep loss (tf)	$\Delta F_3 = E_p \cdot A_p \cdot \epsilon_{Creep}$
	drying shrinkage loss (tf)	$\Delta F_4 = E_p \cdot A_p \cdot \epsilon_s$

Here, E_p : Young's modulus of tendon
 A_p : Sectional area of tendon
 $\Delta \epsilon$: Amount of changes in strain of the structure at tendon tensioning calculated by FEM method
 $\Gamma(t)$: Relaxation coefficient from the LARSON-MILLER method³⁾
 F_0 : Average initial (at time of anchoring) tensile force of tendon
 ϵ_{Creep} : concrete creep strain calculated with equations (5), (6)
 ϵ_s : concrete drying shrinkage strain calculated with equation (7)

Comparison of lift-off force measurements and the calculated residual tensile force of tendons are shown in Table 2 and Fig.6, and Table 3 shows the items within the calculation.

Here, lock-off force subtracted by the total of four factors $\Sigma \Delta F_i$ which dominates the decrease in tendon tensile force being elastic loss (ΔF_1), relaxation loss (ΔF_2), creep loss (ΔF_3) and drying shrinkage loss (ΔF_4), describes the residual tensile force of tendon.

As can be seen in Table 2, the results of (measurement/calculation) ratio were 0.98~1.02 for the first year ISI, 0.99~1.06 for the third year ISI, 0.98~1.06 for the fifth year ISI, 0.99~1.06 for the tenth year ISI, and the measurement and calculation results showed good correspondence. However, lift-off force measurement is actually tensile force detected at the tendon anchoring ends and on the other hand the calculation results correspond to the amount of changes in average tendon tensile force. Of the measured lift-off forces, there are measurements that have a some range in the fluctuating amount of tensile force at the tendon ends and also those that show increase in tensile force which should have declined. These are the effects of redistribution of tensile force caused by non-uniform friction force and the effects due to redistribution of tensile force⁴⁾ is approximately 2 to 3% of the initial tensile force at tendon ends. Therefore, although the (measurement/calculation) ratio of tendon end tensile force at the first year to the tenth year ISI are 0.98~1.06, with the consideration of

measurement errors and effects due to redistribution of tensile force, it can be said that the properties of the measured residual tendon tensile force and the calculation results show good correspondence.

7. CONCLUDING REMARKS

Conclusions as hereunder are made from the test results and strain together with other measurement results derived from ISI tests performed up to the tenth year on the PCCV of Tsuruga Unit No.2.

- (1) There were no abnormality detected from visual inspection and grease testing.
- (2) The fluctuation characteristics of creep and drying shrinkage strain are affected by environmental factors (especially relative humidity). The calculation results with the evaluation method considering this effect and measurements are nearly concurrent.
- (3) From the comparison of measurement of residual tensile force (lift-off force) and calculation results (calculated various loss subtracted from lock-off force) the measurement/calculation ratio are 0.98~1.06.
- (4) With the consideration of measurement errors and redistribution of tensile force, the characteristics of measured residual tensile force of tendon and the calculated results confirmed the behavior of residual tensile force of tendon to be as expected.

References

- 1) *Standard Specification on Prestressed Concrete*, Japan Society of Civil Engineering, 1978
- 2) Y.Watanabe, K.Kawai, S.Akita, Y.Sono, T.Yamaguchi, M.Yamamoto,etc., In-service inspection and R&D of PCCVs in Japan. *Proc. of JOINT WANO/OECD -NEA workshop, Prestress Loss in NPP Containment*, PP 151-186,Poitiers, France, August 1997
- 3) F.R.Larson, J.Miller. A Time-Temperature Relationship for Rupture and Creep Stress, *Trans. of ASME*, PP 765-775, July 1952
- 4) A. Kato, T.Abe, Y.Sono, T.Yamaguchi, M.Yamamoto, Study on the tensile force Redistribution of heated tendon, *Transaction of the 14th SMIRT*, H01/6, 1997

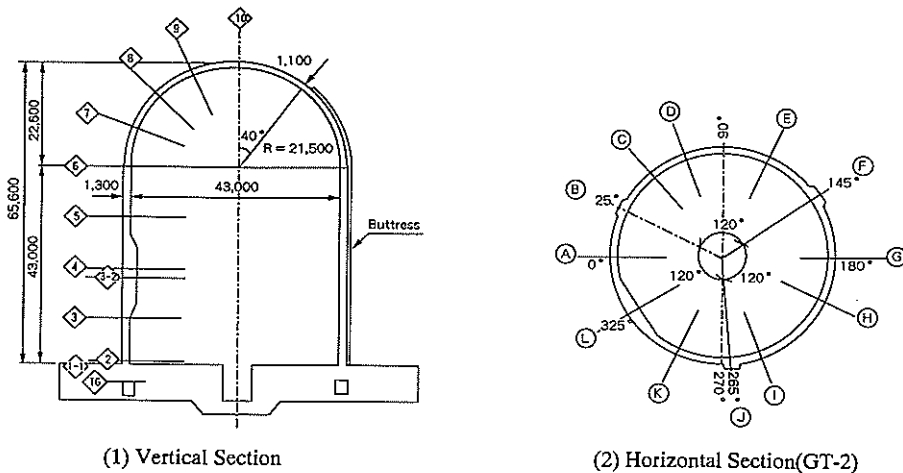


Fig.1 Dimension of PCCV and location of strain measurements

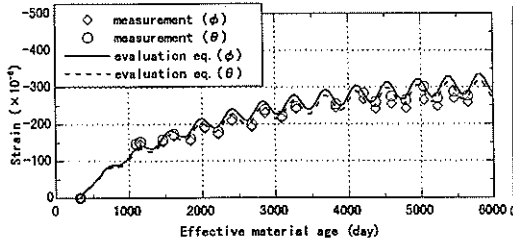


Fig. 2 Long term behavior of strain due to secular changes (Average of section 9 and 10)

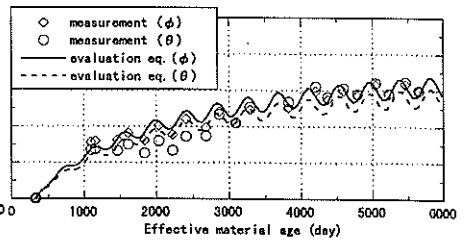


Fig. 3 Long term behavior of strain due to secular changes (Average of section 7 and 8)

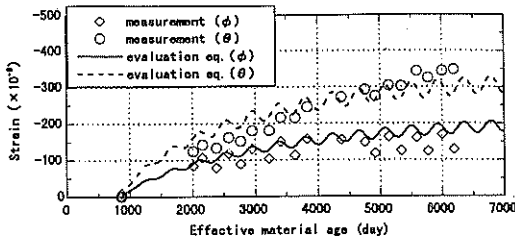
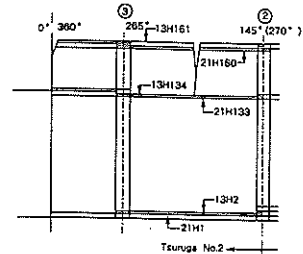
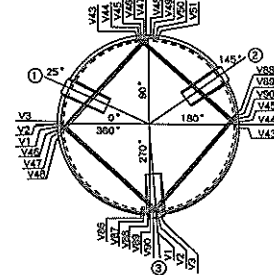


Fig. 4 Long term behavior of strain due to secular changes (Section 3)



(1) Hoop Tendons



(2) Inverted U Tendons

Table 2 Measurements and calculations of tendon lift-off force

Inspected tendon	Anchoring load at tensioning (ton)	First year ISI		Third year ISI		Fifth year ISI		Tenth year ISI			
		Measurement ① (ton)	Calculation ② (ton)	①/②	Measurement ① (ton)	Calculation ② (ton)	①/②	Measurement ① (ton)	Calculation ② (ton)	①/②	
Cylinder hoop tendon	H5	691	653	651.0	1.00						
	H10	690						650	630.7	1.03	
	H25	699				654	635.3	1.03			
	H37	689	627	619.6	1.01	632	610.5	1.03	622	605.4	1.03
	H44	689				630	616.6	1.02			
	H54	690							633	631.7	1.00
	H58	682	644	633.5	1.02						
	H56	693							616	612.2	1.01
	H102	669	634	644.7	0.96	636	636.2	1.00	627	630.7	0.99
	H115	666				641	619.9	1.04			
H119	652	636	650.6	0.98							
Dome hoop tendon	H141	697	649	664.8	0.96	650	656.9	0.99	639	651.9	0.98
	H150	679				631	635.0	0.99			
	H157	687							651	629.8	1.03
Inverted U tendon	V161	690	631	642.2	0.98						
	V16	687	655	659.7	0.99						
	V23	691	661	664.9	1.01	663	646.8	1.02	653	643.6	1.01
	V31	689				655	644.3	1.02	645	629.1	1.01
	V50	693							652	636.9	1.02
	V56	668	655	649.5	1.01						
	V63	666				691	648.0	1.05	666	642.8	1.04
	V82	690				677	640.4	1.06			
	V85	693	663	658.0	1.01						

Fig. 5 Location of tendons

Table 3 Items within the calculation of residual tensile force of tendon

Lock-off	Meas.	Calculated Values																		
		No. 1 ISI T_1				No. 2 ISI T_2				No. 3 ISI T_3				No. 4 ISI T_4						
		Cal. Tension Loss				Residual Tendon Force				Cal. Tension Loss				Residual Tendon Force						
	ΔF_1	ΔF_2	ΔF_3	ΔF_4		ΔF_1	ΔF_2	ΔF_3	ΔF_4		ΔF_1	ΔF_2	ΔF_3	ΔF_4		ΔF_1	ΔF_2	ΔF_3	ΔF_4	
Cylinder Hoop Tendon	H5	691	1.7	7.8	25.8	4.0	651.6	--	--	--	--	--	--	--	--	--	--	--	--	--
	H10	680	7.4	--	--	--	--	--	--	8.6	34.1	9.2	630.7	--	--	--	--	--	--	--
	H25	699	17.3	--	--	--	8.4	31.1	6.9	635.3	--	--	--	--	--	--	--	--	--	--
	H37	689	31.7	7.8	25.8	4.0	619.6	8.4	31.1	6.9	610.9	6.6	34.1	9.2	605.4	8.8	37.5	12.3	598.7	--
	H44	689	27.0	--	--	--	8.4	31.1	6.9	615.6	--	--	--	--	--	--	--	--	--	--
	H54	690	6.5	--	--	--	--	--	--	--	8.6	33.6	9.2	631.7	--	--	--	--	--	--
	H58	682	11.1	7.9	25.4	4.0	633.8	--	--	--	--	--	--	--	--	--	--	--	--	--
	H80	693	29.3	--	--	--	--	--	--	--	8.8	33.8	9.2	612.1	--	--	--	--	--	--
	H102	689	6.8	7.9	25.5	4.0	644.8	8.4	30.8	6.9	636.1	8.6	33.8	9.2	630.6	8.8	37.1	12.3	624.0	--
	H115	686	21.0	--	--	--	8.4	30.8	6.9	618.9	--	--	--	--	--	--	--	--	--	--
Dome Hoop Tendon	H119	692	10.4	8.1	18.7	4.0	650.8	--	--	--	--	--	--	--	--	--	--	--	--	--
	H141	697	2.9	6.2	16.6	4.8	654.5	8.7	20.3	8.2	656.9	9.0	22.4	10.9	651.8	9.2	24.6	14.6	645.7	--
	H150	679	6.6	--	--	--	8.7	20.3	8.2	635.0	--	--	--	--	--	--	--	--	--	--
	H157	697	6.5	--	--	--	--	--	--	--	8.7	30.0	10.9	631.1	--	--	--	--	--	--
	H161	690	11.8	8.1	22.3	4.8	643.0	--	--	--	--	--	--	--	--	--	--	--	--	--
Inverted U Tendon	V16	687	-0.1	8.5	14.4	4.0	660.2	--	--	--	--	--	--	--	--	--	--	--	--	--
	V23	681	8.7	8.5	14.4	4.0	655.4	9.0	17.2	6.8	645.3	8.3	19.5	9.4	644.1	9.6	20.6	12.0	640.1	--
	V31	688	10.2	--	--	--	9.0	17.2	6.8	644.8	9.3	19.5	9.4	639.6	--	--	--	--	--	--
	V50	693	17.4	--	--	--	--	--	--	9.3	19.5	9.4	637.4	--	--	--	--	--	--	--
	V59	685	11.1	8.5	14.4	4.0	655.0	--	--	--	--	--	--	--	--	--	--	--	--	--
	V63	688	6.5	--	--	--	9.0	17.2	6.8	645.5	9.3	19.5	9.4	643.3	9.6	20.6	12.0	639.3	--	--
	V82	650	16.1	--	--	--	9.0	17.2	6.8	640.9	--	--	--	--	--	--	--	--	--	--
	V85	693	7.6	8.5	14.4	4.0	658.5	--	--	--	--	--	--	--	--	--	--	--	--	--

Note : T_0 : Lock-off force of tendon (average of S and F side anchoring tension ; tonf)
 T_1, T_2, T_3, T_4 : Lift of force at 1st, 3rd, 5th, 10th year ISI respectively (tonf)
 ΔF_1 : Elastic deformation (tonf)
 ΔF_2 : Relaxation of Tendon (tonf)
 ΔF_3 : Creep (tonf)
 ΔF_4 : Shrinkage (tonf)
 Calculated residual tendon force ②~⑤ are results of lock-off measurements subtracted by total calculated loss

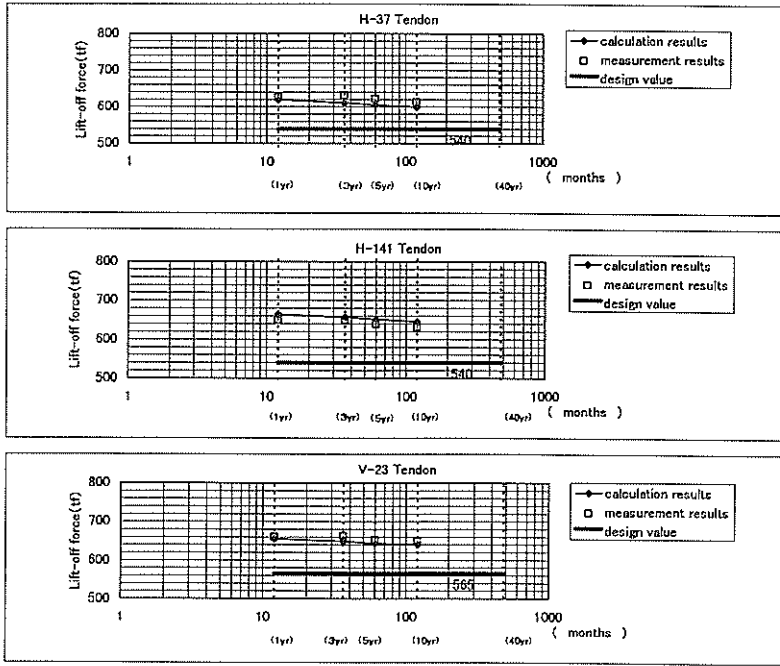


Fig.6 Measurements and calculations of tendon lift-off force